Cholesterol Metabolism — Impact for SARS-CoV-2 Infection Prognosis, Entry, and Antiviral Therapies

Congwen Wei[1,7], Luming Wan[1,7], Yanhong Zhang[1,7], Chen Fan[2,7], Qiulin Yan[1], Xiaoli Yang[3], Jing Gong[1], Huan Yang[1], Huilong Li[1], Jun Zhang[1], Zhe Zhang[1], Rong Wang[1], Xiaolin Wang[1], Jin Sun[1], Yulong Zong[4], Feng Yin[5], Qi Gao[6]*, Yuan Cao[2]* and Hui Zhong[1]*

1 Beijing Institute of Biotechnology, Beijing, 100850, China.

2 Department of Laboratory Medicine, the 960th Hospital of PLA, Jinan, 250031, China.

3 Department of Clinical Laboratory, the Third Medical Centre, Chinese PLA General Hospital, 100850, China.

4 Department of Laboratory Medicine, Taian City Central Hospital, Taian, 271000, China.

5 Department of Laboratory Medicine, Taian City Central Hospital Branch, Taian, 271000, China.

6 Hotgen Biotech Co., Ltd. Beijing, 102600, China.

7 These authors contributed equally to this work

*Correspondence : gaoqi@hotgen.com(Q.G.); labs.net@gmail.com(Y.C.); towall@yahoo.com(H.Z.).

Running title: SARS-CoV-2 modulates the cholesterol metabolism

Abstract

The recently emerged pathogenic SARS-coronavirus 2 (SARS-CoV-2) has spread rapidly, leading to a global pandemic. Identification of risk factors for morbidity and cellular coreceptors for SARS-CoV-2 entry is thus urgently needed. In this study, we performed a retrospective study involving 861 patients with COVID-19 from a single-center classified as mild, moderate, severe or critical and found that SARS-CoV-2 infection was associated with clinically significant lower levels of cholesterol. The levels of both TC and HDL were inversely associated with the severity of SARS-CoV-2 infection. In addition, in patients with severe disease, a significant increase in the serum HDL level was correlated with good outcomes. We also showed that a clinically approved HDLR antagonist inhibited SARS-CoV-2 pseudovirus infection. Notably, SARS-2-S bound to cholesterol. Our results not only identify the HDL level as a prognostic marker for SARS-CoV-2 infection but also indicate a potential target for antiviral intervention.

Introduction

Since the outbreak of COVID-19 caused by severe acute respiratory syndrome coronavirus 2 (SARS-CoV-2), more than a million SARS-CoV-2 cases have been reported in over 200 countries [1]. The diameter of SARS-CoV-2 virions is roughly 90 to 120 nm and four structural proteins are encoded within the intact virions, including the spike (S) protein, nucleocapsid (N) protein, envelope (E) protein, and membrane (M) protein[2].

There are two primary entry pathways for enveloped viruses into host cells, some viruses use their envelopes to fuse with the plasma membrane at the cell surface, whereas others take advantage of the cell's endocytic machinery [3,4]. Although most viruses use only one of these pathways to enter cells, some viruses use multiple mechanisms to gain entry into host cells [4]. The entry of SARS-CoV into cells occurred by direct fusion at the plasma membrane and endocytic pathway. SARS-CoV-2 is closely related to SARS-CoV, with ~76% amino acid identity. Both viruses use angiotensin-converting enzyme 2 (ACE2) as the entry receptor and employ the cellular serine protease TMPRSS2 for S protein priming [5]. In addition to ACE2, CD147 facilitates SARS-CoV-2 entry into host cells; however, other coreceptors or cellular molecules may be required to facilitate SARS-CoV-2 entry [6].

Cholesterol homeostasis is vital for proper cellular and systemic functions. Excess cholesterol are either stored as cytosolic lipid droplets or released as plasma lipoproteins including chylomicrons and VLDL, LDL and HDL cholesterol. LDL cholesterol can be taken up by the liver and extrahepatic tissues via the LDL receptor

(LDLR), which is nearly ubiquitously expressed, whereas HDL cholesterol is transported back to the liver for scavenger receptor class B type I-mediated uptake. Dysregulated cholesterol homeostasis underlies cardiovascular disease, neurodegenerative diseases and cancers [7]. Interestingly, dysregulation of lipid metabolism in viral infection has been suggested. Hepatitis C virus (HCV) infection is associated with reduced serum LDL levels. LDLR and scavenger receptor B1 (SR-B1) are candidate receptors HCV entry into hepatocytes [8].

Alterations in serum lipid levels in the context of SARS-CoV-2 infection have seldom been reported [9]. In this study, we performed a retrospective study involving 861 patients with COVID-19 classified as mild, moderate, severe or critical. The serum concentrations of both TC and HDL-C can be used as indicators of disease severity and prognosis in COVID-19 patients. Mechanistically, SARS-2-S bound to cholesterol. The HDLR inhibitor ITX 5061 inhibited SARS-CoV-2 pseudovirus infection and might constitute a treatment option at the early stage of infection.

Experimental Procedures

Materials

His-tagged SARS-CoV-2 Spike (SARS-CoV-2-S) recombinant proteins were purchased from Sino Biological Inc. (40589-V08B1). ITX 5601 was purchased from MedChemExpress Inc. (HY-19900). HDL was purchased from Sigma-Aldrich Inc. (L8039).

Data sources

This study was approved by the Ethics Committee of the TaiKang Tongji hospital ([2020] TKTJLL-003). As we collected the data from electronic medical files without contacting with the patients directly or analyzing the serum, written informed consent was waived. The basic informations and serum biochemical test results were collected from 861 patients with COVID-19 in TaiKang Tongji Hospital (Wuhan, Hubei province, People's Republic of China) from February 16 to March 20, 2020. Serum lipid profiles from 1108 age- and sex-matched individuals from the Third Medical Center of Chinese PLA General Hospital were used as reference values.

Clinical manifestations were used to classify the disease status into four categories: mild, moderate, severe and critical. Mild clinical disease was characterized by mild symptoms with no pulmonary inflammation visible upon imaging. Disease was classified as moderate in the overwhelming majority of patients, who showed symptoms of respiratory infection, such as fever, cough, and sputum production, with pulmonary inflammation visible upon imaging. Disease was classified as severe when symptoms of dyspnea appeared, as assessed by the following symptoms: shortness

of breath, respiration rate (RR) ≥ 30 bpm, resting blood oxygen saturation ≤ 93%, partial pressure of arterial oxygen/fraction of inspired oxygen ratio (PaO_2/FiO_2) ≤ 300 mmHg, or pulmonary inflammation that progressed significantly (> 50%) within 24 to 48 hours. Critical disease was classified as the presence of respiratory failure, shock, or organ failure that required intensive care. Infection was confirmed in all patients by viral detection using quantitative RT-PCR, which simultaneously ruled out infection by other respiratory viruses, such as influenza virus A, influenza virus B, Coxsackie virus, respiratory syncytial virus, parainfluenza virus and enterovirus. All cases were diagnosed and classified according to the New Coronavirus Pneumonia Diagnosis Program (6th edition) published by the National Health Commission of China. Among the patients with COVID-19, 216 cases were classified as mild, 363 as moderate, 217 as severe and 65 cases as critical (Table S1).

Cell lines

293T (human kidney), HeLa (human ovarian), and Vero (African green monkey kidney) cells were incubated in Dulbecco's modified Eagle's medium (Gibco). HeLa cells stably expressing human ACE2 were generated by transfection and puromycin-based selection. All cell lines were incubated at 37°C and 5% CO_2 in a humidified atmosphere and had previously been tested for mycoplasma contamination. Lipofectamine 2000 (Invitrogen) reagent was used for transfection following the manufacturer's protocol.

Plasmids

Codon-optimized cDNA encoding SARS-CoV-2-S (QHU36824.1) with a C-terminal 19

amino acid deletion was synthesized and cloned into the eukaryotic expression vector pcDNA3.1 (Invitrogen). Expression plasmids for human ACE2 were cloned into pcDNA3.1 (Invitrogen). A QuickChange™ Mutagenesis Kit (Stratagene) was used to generate the expression plasmids for SARS-CoV-2-S mutants.

Pseudotyped virus infection assays

The SARS-CoV-2 pseudotyped virus was produced by a similar method which was described previously [10]. Briefly, 12 μg pNL4-3.Luc.E−R− and 6 μg pcDNA3.1-SARS-CoV-2-S were co-transfected into 293T cells and the pseudotyped virus was purified to infect cells. The cells were lysed at 48 h post-infection and Wallac Multilabel 1450 Counter (Perkin–Elmer, Singapore) was used to measure luciferase signal. The relative light units for each condition were reported as the mean plus or minus the standard error of the mean for the 3 wells.

In order to block HDLR on the cell surface, 100 μL of serially diluted ITX 5061 (MedChemExpress, HY-19900) solutions was added into HeLa cells in a 96-well plate. Subsequently, 100 μL of pseudotyped virus was added onto the cells (MOI, 5). After co-incubation for 72 hours, Renilla luciferase expression was determined by measuring the activity of firefly luciferase in cell lysates using a luciferase reporter kit (Promega, E6120) and a multimode microplate reader (Tecan).

Immunoblot analysis

Cell lysates were prepared in lysis buffer (50 mM Tris-HCl [pH 7.5], 150 mM NaCl, 1 mM phenylmethylsulfonyl fluoride, 1 mM dithiothreitol, 10 mM sodium fluoride, 10 mg/ml aprotinin, 10 mg/ml leupeptin, and 10 mg/ml pepstatin A) containing 1%

Nonidet P-40. Soluble proteins were subjected to SDS-PAGE and immunoblotting with the indicated antibodies. Antigen-antibody complexes were visualized by chemiluminescence (PerkinElmer).

Microscale thermophoresis (MST)

MST assay was conducted as previously described [11]. In brief, S protein samples were and labeled and mixed with cholesterol in binding buffer at indicated concentrations at room temperature. Fluorescence was determined in a thermal gradient generated by a Monolith NT.115 from NanoTemper Technologies and the data analyzed by MOAffinityAnalysis v2.1.23333.

Statistical methods

In this study, GraphPad 6.0 software was used for data statistics and mapping. Continuous variables were presented as mean ± standard deviation and categorical variables were described as frequencies. Continuous variables were compared using independent group t tests or Mann-Whitney U test. Chi-square tests were used for categorical variables. Above statistical analyses were two-sided and significance values were set at * $P < 0.05$, ** $P < 0.01$, and *** $P < 0.001$.

Acknowledgements

This study was supported in part by grants from the National Key Research and Development Program of China (2018YFA0900800) and the National Natural Science Foundation of China (31670761, 31872715 and 81773205). The funders had no role in the study design, data collection and analysis, decision to publish, or preparation of the manuscript.

Conflict of interests

The authors have declared that no competing interests exist.

Results

Clinical characteristics of the patients

The study population comprised patients in TaiKang Hospital (Wuhan, Hubei province, People's Republic of China) between February 16, 2020 and March 20, 2020. The median age was 60 years (range, 16-96 years); 386 were men and 475 were women. The reference population comprised patients in the Third Medical Center of Chinese PLA General Hospital between March 1, 2018 and April 1, 2019. The median age was 61 years (range, 31-96 years), and this population comprised 481 men and 627 women. The clinical and biochemical characteristics of these individuals are given in Table S1. The age and sex distributions did not differ between these two groups.

SARS-CoV-2 infection is associated with clinically significant lower levels of TC and HDL cholesterol

Liver damage and various digestive symptoms in patients infected with SARS-CoV-2 prompted us to investigate whether infection with this virus could lead to alterations in lipid metabolism. The serum lipid levels of each subject were measured. Total TG levels were similar between the reference population and the SARS-CoV-2-infected patients (P=0.062; Table S1 and Figure 1A), but the serum TC and HDL levels were significantly lower in patients infected with SARS-CoV-2 than in the reference population (P< 0.0001 and P<0.0001, respectively; Table S1 and Figure 1B-C). Thus, SARS-CoV-2 infection was associated with clinically significant lower levels of TC and HDL. Interestingly, patients with SARS-CoV-2 infection had significantly higher serum LDL levels than age- and sex-matched adults from the reference population (P<

0.0001; Table S1 and Figure 1D).

Cholesterol levels are inversely associated with disease severity in patients infected with SARS-CoV-2

We next sought to determine whether serum lipid levels were correlated with disease conditions in patients with SARS-CoV-2 infection. Although serum TG levels were significantly lower in patients with moderate disease than in those with mild disease (P< 0.0001; Table S2 and Figure 2A), they were similar in moderately, severely and critically ill patients (Table S2 and Figure 2A). However, the serum TC (Table S2 and Figure 2B), HDL (Table S2 and Figure 2C) and LDL (Table S2 and Figure 2D) concentrations were negatively correlated with disease severity and were particularly lower in critically ill patients than in patients with less severe disease. Specifically, the median HDL concentration in critically ill patients was 0.888 mmol/L (Table S2), which was below the normal range (1.03-1.89 mmol/L). Collectively, these results indicate that serum cholesterol levels may reflect the disease progression in patients infected with SARS-CoV-2.

TC and HDL levels have prognostic value for patients with severe disease associated with SARS-CoV-2 infection

We then selected 100 patients with severe symptoms but a cured outcome (survivors) and 16 with severe symptoms that died (nonsurvivors) and compared their lipid levels at admission (pre-therapy) and after therapy (post-therapy). Although both groups of patients showed similar TG levels before and after therapy (Figure 3A), the TC and HDL levels of survivors rose significantly after therapy but

dropped significantly in nonsurvivors (Figure 3B-C). LDL levels remained unchanged in survivors but decreased significantly after therapy (Figure 3D). In addition, we randomly selected 11 survivors and 9 nonsurvivors and monitored dynamic changes in the HDL level of each patient from disease onset to recovery or death. Although the disease course differed in each patient, the HDL level increased progressively in 8 out of 11 survivors (Figure 3E), whereas the HDL level in all nonsurvivors showed a progressive decreasing trend (Figure 3F). Taken together, these results suggest that TC and HDL levels are prognostic predictors in patients with severe disease caused by SARS-CoV-2 infection.

An HDLR antagonist blocks SARS-CoV-2 infection

Our results showed that SARS-CoV-2 infection led to reduced HDL levels in patients, which increased progressively after successful treatment; thus, we speculated that SARS-2-S might manipulate the reverse cholesterol transport (RCT) pathway for its entry. To this end, we employed ITX 5061, a potent SR-B1 antagonist that can increase HDL levels, and assessed its effect on SARS-CoV-2 infection. Accordingly, pretreatment of 293T cells with ITX 5061 in the presence of HDL strongly inhibited the entry of SARS-2-S pseudovirus into host cells (Figure 4A), with an EC50 of 520 nM. To assess the cytotoxicity of ITX 5061, we evaluated its effect on cell survival. Treatment with the indicated dose of ITX 5061 did not affect cell survival (Figure 4B). These data show that the HDLR antagonist significantly inhibits SARS-CoV-2 infection in vitro.

SARS-2-S binds to cholesterol

The observation that SARS-2-S manipulates the SR-B1 pathway for its entry prompted us to investigate the possible interaction of SARS-2-S with lipoprotein or cholesterol. A search for cholesterol-regulated motifs in the primary sequence of SARS-2-S identified 6 putative cholesterol recognition amino acid consensus (CRAC) motifs adjacent to the inverted cholesterol recognition motif called CARC (Figure 5A)[12]. To evaluate the ability of SARS-2-S to bind to cholesterol, we purchased purified soluble SARS-2-S proteins. These proteins were incubated with cholesterol in 0.1% Fos-choline 13 at concentrations ranging from 0.1 to 1000 nM, and interactions were assessed using MST. SARS-2-S interacted with cholesterol with an EC50 of 187.6±120.5 nM (Figure 5B). These data indicate that SARS-CoV-2 may manipulate cholesterol metabolism via the SARS-2-S-cholesterol interaction.

Discussion

The present study provides evidence that SARS-CoV-2 infection is intimately connected with alterations in circulating cholesterol levels. The levels of both TG and HDL were significantly lower in patients with severe disease than in patients with moderate or mild disease. After successful treatment, cholesterol metabolism was reestablished in patients with SARS-CoV-2 infection. Mechanistically, SARS-2-S binds to cholesterol. Binding of SARS-2-S to cholesterol may ensure particle infectivity and can be blocked by ITX 5061, a clinically approved SR-B1 antagonist [13]. These findings suggest that SARS-CoV-2 orchestrates cholesterol metabolism to support its entry. Our results not only identify serum cholesterol as a risk factor for morbidity of disease caused by SARS-CoV-2 infection but also reveal a potential target for therapeutic intervention.

Specific lipid profile alterations are associated with several viral infections, including severe dengue, HIV, and HCV infections [14-16]. In this study, we specifically addressed the connection between the SARS-CoV-2 virus, a vector-borne pathogen responsible for a global epidemic, with host cholesterol metabolism. The serum concentrations of both TC and HDL can be used as indicators of disease severity and prognosis in COVID-19 patients. Interestingly, although decreasing levels of LDL were associated with disease progression, SARS-CoV-2-infected patients had significantly higher levels of LDL than normal adults matched for age and sex. Our unpublished data confirmed this result in SARS-CoV-2-infected patients from another hospital in Hubei. However, more data are needed to reveal the mechanism underlying the association

of increased LDL levels with SARS-CoV-2 infection.

Several possible mechanisms could lower the circulating HDL levels as a result of SARS-CoV-2 infection. Here, we presented data showing specific enhancement of SARS-CoV-2 infection in the presence of HDL. Considering the reduced HDL levels, we speculated that HDL-virus particle interactions may facilitate viral entry through the uptake of lipoprotein particles. SARS-2-S contains multiple CRAC motifs and CARC motif. Although these motifs alone might have low predictive value for identifying cholesterol-binding sites, the MST assay results confirmed the ability of SARS-2-S to bind cholesterol. The possible interaction of SARS-2-S with lipoprotein and other mechanism involved in the reduced HDL levels will reveal more clues of the virus transmission routes and its potential pathogenesis.

Immune dysfunctions, including lymphopenia, decreases in CD4+ T-cell levels, and abnormal cytokine levels, are a common feature in cases of SARS-CoV-2 infection and might be critical factors associated with disease severity [17]. We speculated that the immune-mediated cytokine storm might result at least partially from decreased HDL levels. HDL relieves cells of excessive amounts of cholesterol and has strong anti-inflammatory properties. In addition, HDL inhibits TLR-induced production of proinflammatory cytokines by macrophages [18]. Moreover, modulation of cellular cholesterol levels by HDL may also affect antigen presentation and the induction of the adaptive immune response [19]. The correlation of reduced HDL levels with disease severity and mortality associated with SARS-CoV-2 infection implies the physiologically important function of HDL. HDL-mediated cholesterol efflux and RCT

become dysfunctional in chronic metabolic diseases such as obesity or atherosclerosis [20,21], consistent with the increased mortality observed in elderly patients and patients with obesity or diabetes. In addition, approximately half of the patients with SARS-CoV-2 infection had chronic underlying diseases, mainly cardiovascular and cerebrovascular diseases and diabetes [2]. Therefore, intensive surveillance and early evaluation of the serum lipid levels in patients with preexisting conditions, especially in older patients with other comorbidities, might be needed.

SR-B1 has been implicated in dengue virus infection. Our results support a role for SR-B1 in cell entry of SARS-CoV-2. SR-B1 is well conserved between species and expressed in many mammalian tissues and cell types, including intestine, macrophages, endothelial cells, smooth muscle cells, keratinocytes, adipocytes, steroidogenic cells and liver. ITX5061, a small-molecule SR-B1 antagonist as a promising inhibitor for HCV infection, also inhibits SARS-CoV-2 infection. Considerable increased expression of SR-B1 is observed in a variety of patients with cancer, who are more susceptible to infection than individuals without cancer, raising the potential advantage for the development of SR-B1 inhibitors for use in SARS-CoV-2 infection.

In conclusion, this study provided key insights into the connection between SARS-CoV-2 infection and cholesterol metabolism and defined potential prognostic and antiviral intervention targets for infections with this virus.

References

1. WHO. Coronavirus disease (COVID-19) Pandemic: World Health Organization.
2. Chen N, Zhou M, Dong X, et al. Epidemiological and clinical characteristics of 99 cases of 2019 novel coronavirus pneumonia in Wuhan, China: a descriptive study. *The Lancet*. 2020;395(10223):507-513.
3. Wang H, Yang P, Liu K, et al. SARS coronavirus entry into host cells through a novel clathrin- and caveolae-independent endocytic pathway. *Cell Res*. 2008;18(2):290-301.
4. Pelkmans L, Helenius A. Insider information: what viruses tell us about endocytosis. *Curr Opin Cell Biol*. 2003;15(4):414-422.
5. Hoffmann M, Kleine-Weber H, Schroeder S, et al. SARS-CoV-2 Cell Entry Depends on ACE2 and TMPRSS2 and Is Blocked by a Clinically Proven Protease Inhibitor. *Cell*. 2020.
6. Wang K, Chen W, Zhou Y-S, et al. SARS-CoV-2 invades host cells via a novel route: CD147-spike protein. 2020.
7. Luo J, Yang H, Song BL. Mechanisms and regulation of cholesterol homeostasis. *Nat Rev Mol Cell Biol*. 2020;21(4):225-245.
8. Catanese MT, Ansuini H, Graziani R, et al. Role of scavenger receptor class B type I in hepatitis C virus entry: kinetics and molecular determinants. *J Virol*. 2010;84(1):34-43.
9. Xingzhong Hu DC, Lianpeng Wu, Guiqing He, Wei Ye. Low Serum Cholesterol Level Among Patients with COVID-19 Infection in Wenzhou,
China. *The Lancet*. 2020.
10. Nie Y, Wang P, Shi X, et al. Highly infectious SARS-CoV pseudotyped virus reveals the cell tropism and its correlation with receptor expression. *Biochem Biophys Res Commun*. 2004;321(4):994-1000.
11. Widenmaier SB, Snyder NA, Nguyen TB, et al. NRF1 Is an ER Membrane Sensor that Is Central to Cholesterol Homeostasis. *Cell*. 2017;171(5):1094-1109 e1015.
12. Fantini J, Di Scala C, Baier CJ, Barrantes FJ. Molecular mechanisms of protein-cholesterol interactions in plasma membranes: Functional distinction between topological (tilted) and consensus (CARC/CRAC) domains. *Chem Phys Lipids*. 2016;199:52-60.
13. Masson D, Koseki M, Ishibashi M, et al. Increased HDL cholesterol and apoA-I in humans and mice treated with a novel SR-BI inhibitor. *Arterioscler Thromb Vasc Biol*. 2009;29(12):2054-2060.
14. Suvarna JC, Rane PP. Serum lipid profile: a predictor of clinical outcome in dengue infection. *Trop Med Int Health*. 2009;14(5):576-585.
15. Funderburg NT, Mehta NN. Lipid Abnormalities and Inflammation in HIV Inflection. *Curr HIV/AIDS Rep*. 2016;13(4):218-225.
16. Hsu CS, Liu CH, Liu CJ, et al. Association of lipid profiles with hepatitis C viral load in chronic hepatitis C patients with genotype 1 or 2 infection. *Am J Gastroenterol*. 2009;104(3):598-604.
17. Zhang C, Shi L, Wang FS. Liver injury in COVID-19: management and challenges. *Lancet Gastroenterol Hepatol*. 2020.
18. De Nardo D, Labzin LI, Kono H, et al. High-density lipoprotein mediates anti-inflammatory reprogramming of macrophages via the transcriptional regulator ATF3. *Nat Immunol*. 2014;15(2):152-160.
19. Wang SH, Yuan SG, Peng DQ, Zhao SP. High-density lipoprotein affects antigen presentation by interfering with lipid raft: a promising anti-atherogenic strategy. *Clin Exp Immunol*. 2010;160(2):137-142.

20. Assmann G, Gotto AM, Jr. HDL cholesterol and protective factors in atherosclerosis. *Circulation*. 2004;109(23 Suppl 1):III8-14.
21. Rashid S, Genest J. Effect of obesity on high-density lipoprotein metabolism. *Obesity (Silver Spring)*. 2007;15(12):2875-2888.

Figure Legends

Figure 1. SARS-CoV-2 infection is associated with clinically significant lower levels of TC and HDL cholesterol

(A-B) TG (A) and TC (B) levels in SARS-CoV-2-infected patients and reference subjects. Differences between the two groups were evaluated using the Mann-Whitney test:

*, $P < 0.05$; **, $P < 0.01$; ***, $P < 0.001$.

(C-D) HDL (C) and LDL (D) levels in SARS-CoV-2-infected patients and reference subjects. Differences between the two groups were evaluated using the Mann-Whitney test:

*, $P < 0.05$; **, $P < 0.01$; ***, $P < 0.001$.

Figure 2. Cholesterol levels are inversely associated with disease severity in patients infected with SARS-CoV-2

(A-B) Plot of TG (A) and TC (B) levels in SARS-CoV-2-infected patients with four different levels of disease severity.

(C-D) Plot of HDL (C) and LDL (D) levels in SARS-CoV-2-infected patients with four different levels of disease severity.

Differences among groups were evaluated using the Mann-Whitney test:

*, $P < 0.05$; **, $P < 0.01$; ***, $P < 0.001$.

Figure 3. TC and HDL levels have prognostic value for patients with severe

SARS-CoV-2 infection

(A-D) Changes in serum TG (A), TC (B), HDL (C) and LDL (D) levels in survivors and nonsurvivors before therapy (pre-therapy) and after therapy (post-therapy).

(E-F) Temporal changes in serum HDL levels in survivors (E) and nonsurvivors (F) starting from illness onset.

Differences between groups were evaluated using the Mann-Whitney test:

*, $P < 0.05$; **, $P < 0.01$; ***, $P < 0.001$.

Figure 4. An HDLR antagonist blocks SARS-CoV-2 infection

(A) HeLa cells stably expressing human ACE2 were preincubated with the indicated concentrations of ITX 5601 in the presence of HDL (300 ng/ml) and subsequently inoculated with pseudovirus particles bearing SARS-2-S. At 48 h postinoculation, pseudotype virus entry was analyzed by determining luciferase activity in cell lysates. Signals of particles bearing no E protein were used for normalization.

(B) HeLa cells stably expressing human ACE2 were preincubated with the indicated concentrations of ITX 5601. At 48 h postinoculation, MTT was added to the cells, and the OD492 value was measured. Signals obtained without ITX 5601 were used for normalization.

Cell-based studies were performed at least three times independently with comparable results. Data are presented as the means ± SEMs. Student's t-test was used for statistical analysis: *, $P < 0.05$; **, $P < 0.01$; ***, $P < 0.001$.

Figure 5. SARS-2-S binds to cholesterol and HDL

(A) Schematic illustration of the cholesterol-binding motif in SARS-2-S. Crucial amino

acid residues in the CARC motif are highlighted in red, crucial amino acid residues in the CRAC motif are highlighted in green, and shared amino acid residues are highlighted in purple. The green stick indicates the CARC motif, and the red stick indicates the CRAC motif.

(B) Effect of cholesterol on fluorescence decay of fluorescently labeled SARS-2-S.

Figure 1

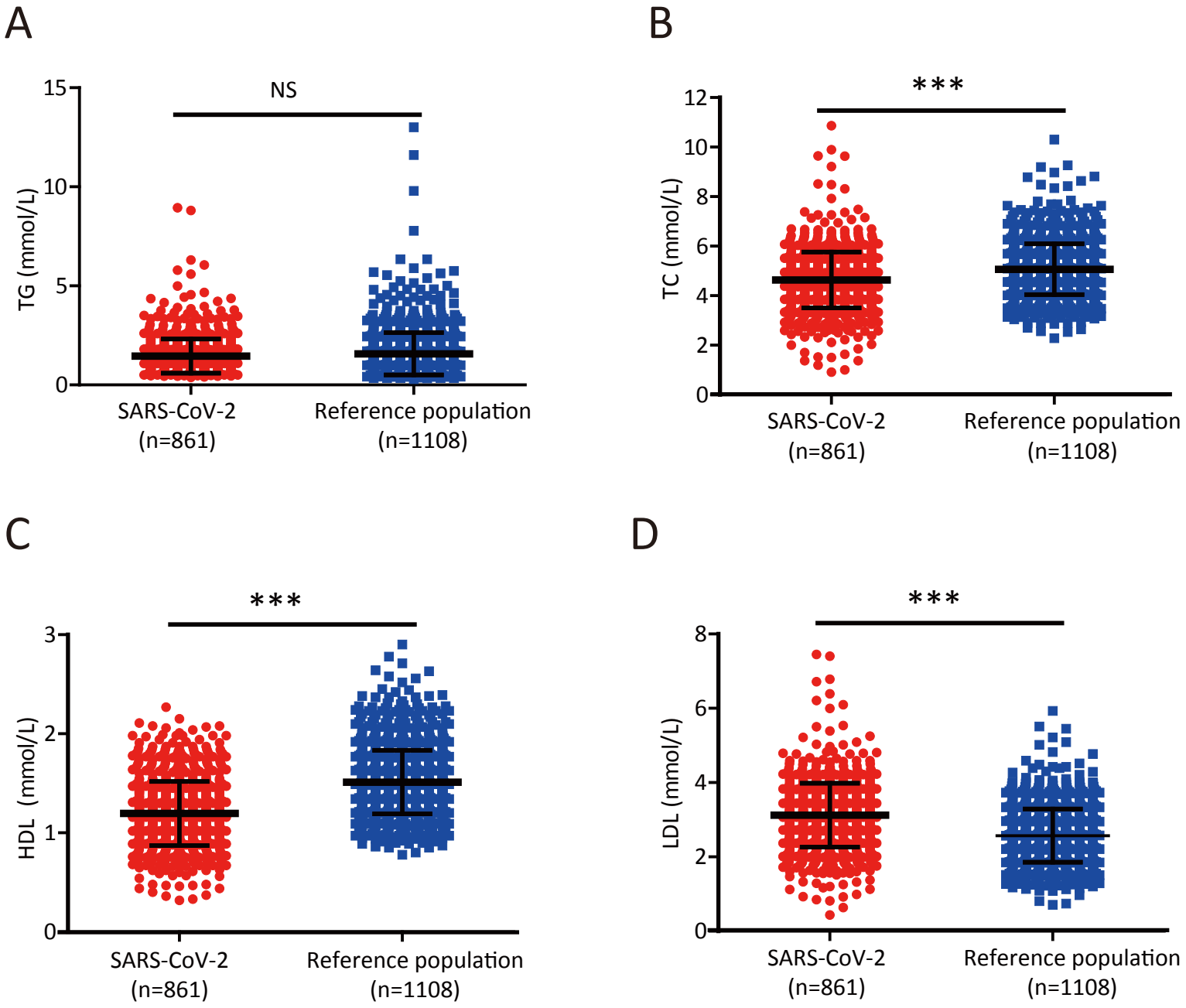
A
NS
TG (mmol/L)
15
10
5
0
SARS-CoV-2
(n=861)
Reference population
(n=1108)
B
***
TC (mmol/L)
12
10
8
6
4
2
0
SARS-CoV-2
(n=861)
Reference population
(n=1108)
C
***
HDL (mmol/L)
3
2
1
0
SARS-CoV-2
(n=861)
Reference population
(n=1108)
D
***
LDL (mmol/L)
8
6
4
2
0
SARS-CoV-2
(n=861)
Reference population
(n=1108)

Figure 2

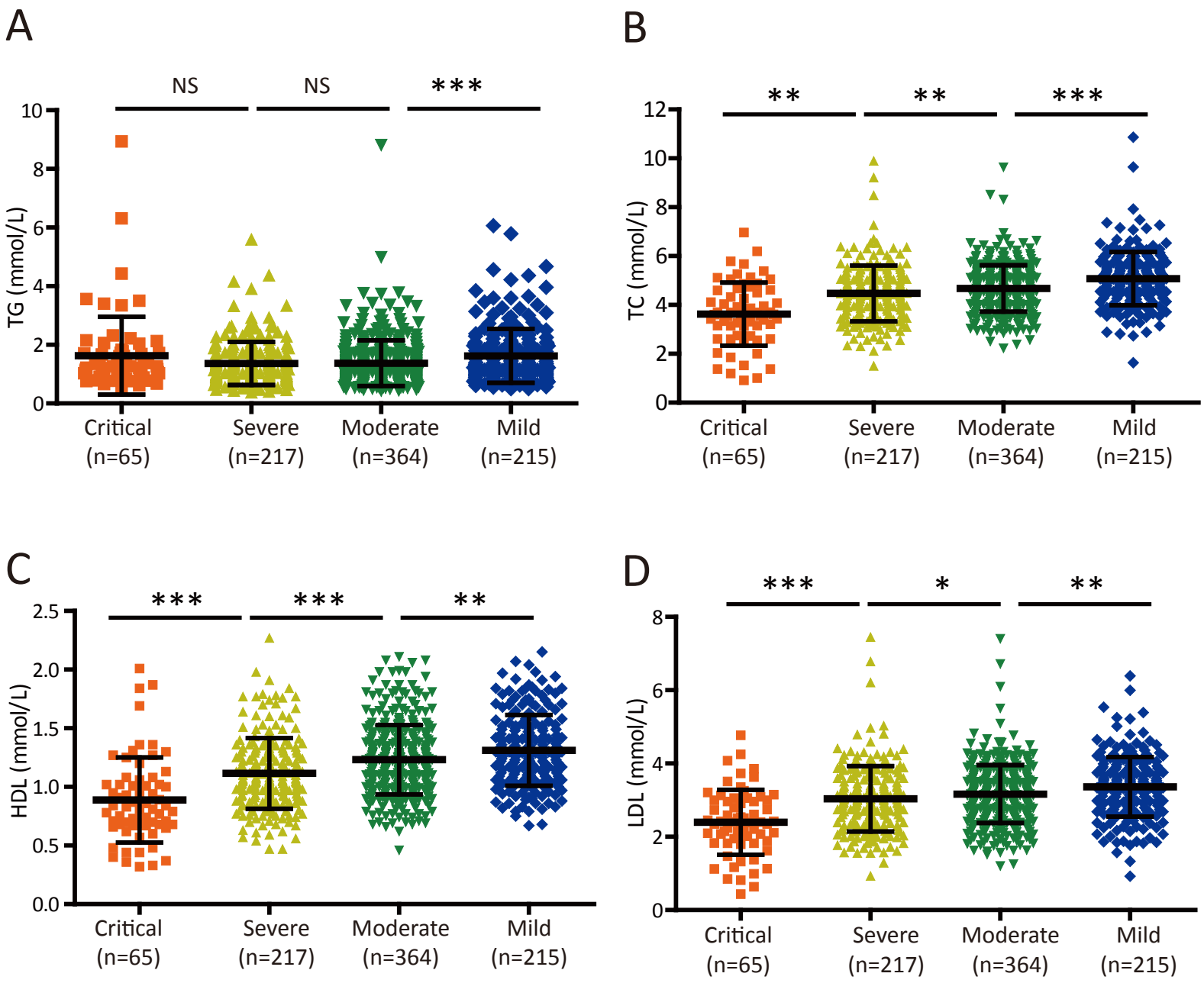
A
NS
NS
***
TG (mmol/L)
10
8
6
4
2
0
Critical (n=65)
Severe (n=217)
Moderate (n=364)
Mild (n=215)
B
**
**
***
TC (mmol/L)
12
10
8
6
4
2
0
Critical (n=65)
Severe (n=217)
Moderate (n=364)
Mild (n=215)
C
***
***
**
HDL (mmol/L)
2.5
2.0
1.5
1.0
0.5
0.0
Critical (n=65)
Severe (n=217)
Moderate (n=364)
Mild (n=215)
D
***
*
**
LDL (mmol/L)
8
6
4
2
0
Critical (n=65)
Severe (n=217)
Moderate (n=364)
Mild (n=215)

Figure 3

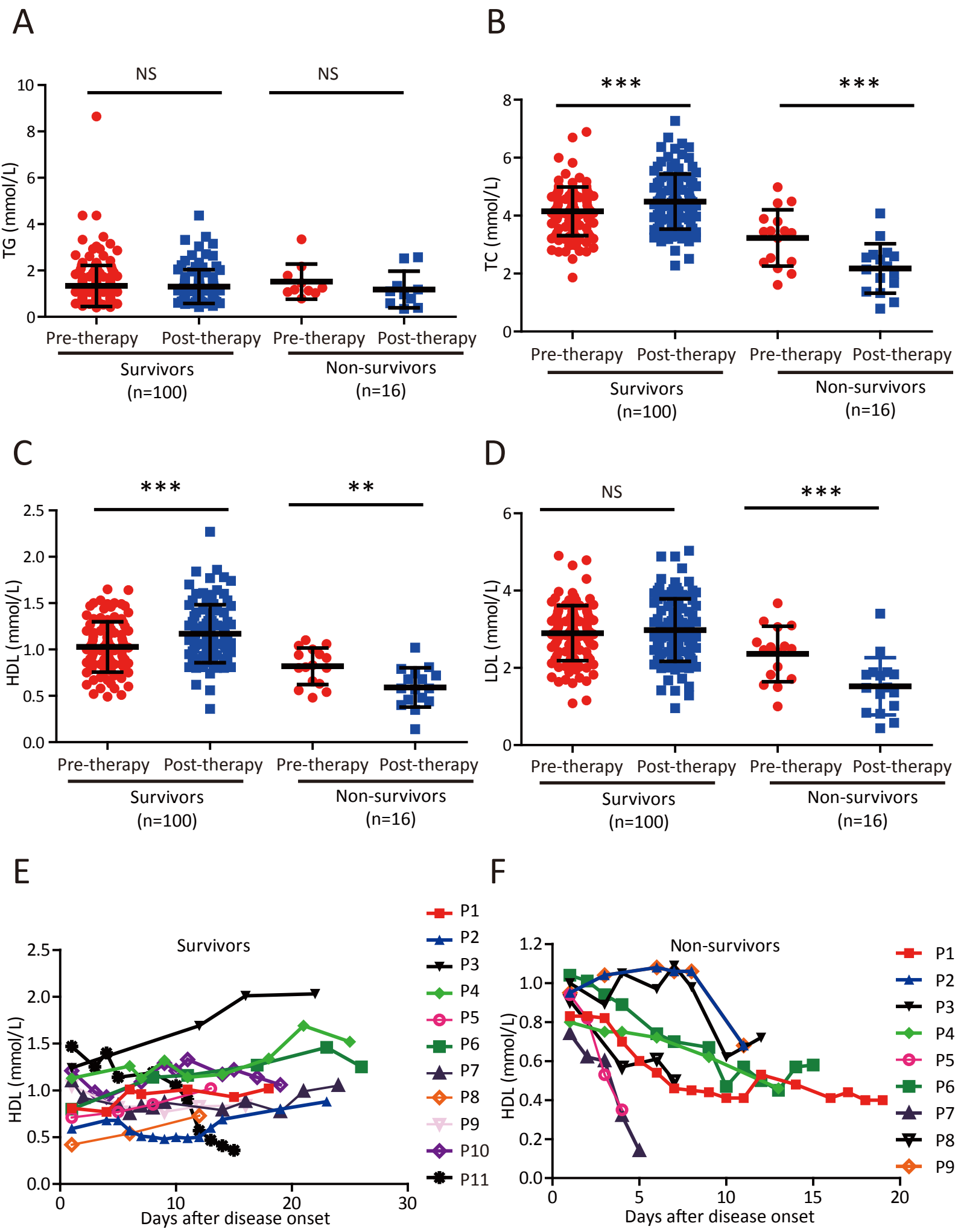
A
NS
NS
TG (mmol/L)
Pre-therapy
Post-therapy
Pre-therapy
Post-therapy
Survivors
(n=100)
Non-survivors
(n=16)
B
***
***
TC (mmol/L)
Pre-therapy
Post-therapy
Pre-therapy
Post-therapy
Survivors
(n=100)
Non-survivors
(n=16)
C
***
**
HDL (mmol/L)
Pre-therapy
Post-therapy
Pre-therapy
Post-therapy
Survivors
(n=100)
Non-survivors
(n=16)
D
NS
***
LDL (mmol/L)
Pre-therapy
Post-therapy
Pre-therapy
Post-therapy
Survivors
(n=100)
Non-survivors
(n=16)
E
Survivors
HDL (mmol/L)
Days after disease onset
P1
P2
P3
P4
P5
P6
P7
P8
P9
P10
P11
F
Non-survivors
HDL (mmol/L)
Days after disease onset
P1
P2
P3
P4
P5
P6
P7
P8
P9

Figure 4

A

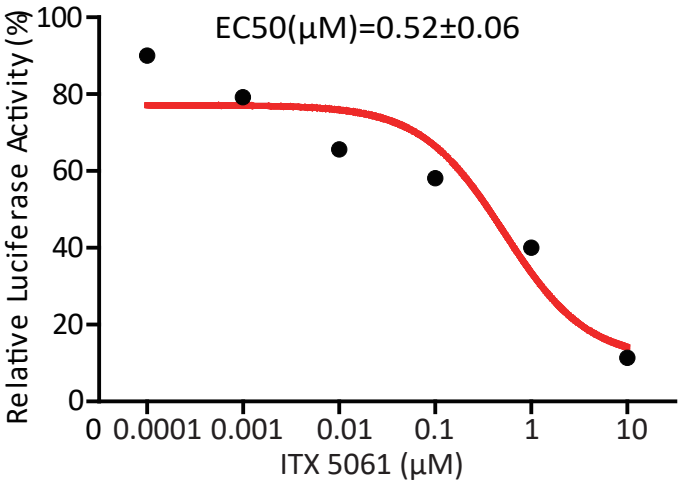
EC50(μM)=0.52±0.06
Relative Luciferase Activity (%)
100
80
60
40
20
0
0
0.0001
0.001
0.01
0.1
1
10
ITX 5061 (μM)

B

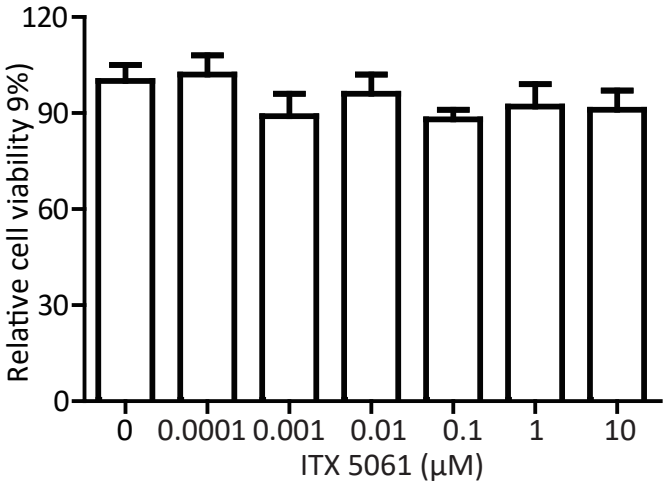
Relative cell viability 9%)
120
90
60
30
0
0
0.0001
0.001
0.01
0.1
1
10
ITX 5061 (μM)

Figure 5

A

SARS-2-S

24-42: LPPAYTNSFTRGVYYPDKV
129-150: KVCEFQFCNDPFLGVYYHKNNK
267-277: VGYLQPRTFLL
445-461: VGGNYNYLYRLFRKSNL (RBD)
776-806: KNTQEVFAQVKQIYKTPPIKDFGGFNFSQIL
1203-1218: LGKYEQYIKWPWYIWL

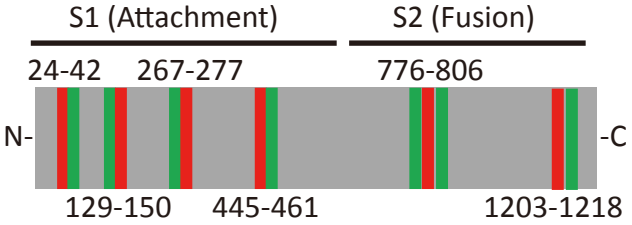

CARC: N-R/K-X(1-5)-F/Y-X(1-5)-L/V-C

CRAC: N-L/V-X(1-5)-Y-X(1-5)-K/R-C
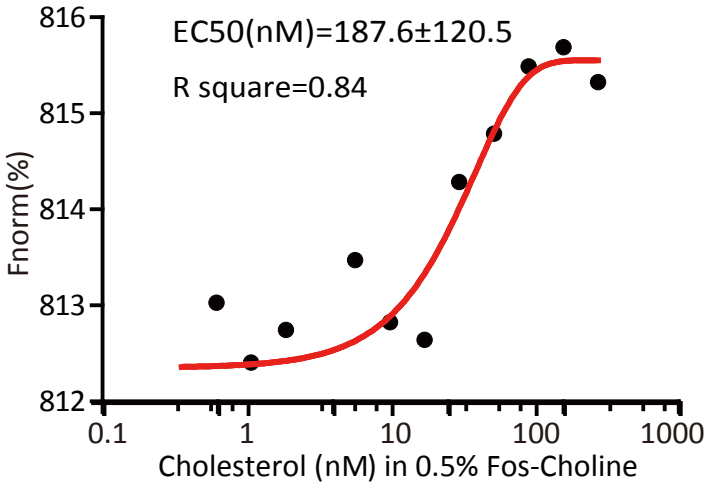
B